



## NRC Publications Archive Archives des publications du CNRC

### **Performance of PEI/BMI semi-IPN membranes for separations of various binary gaseous mixtures**

Kurdi, Jamal; Kumar, Ashwani

This publication could be one of several versions: author's original, accepted manuscript or the publisher's version. / La version de cette publication peut être l'une des suivantes : la version prépublication de l'auteur, la version acceptée du manuscrit ou la version de l'éditeur.

For the publisher's version, please access the DOI link below. / Pour consulter la version de l'éditeur, utilisez le lien DOI ci-dessous.

#### **Publisher's version / Version de l'éditeur:**

<https://doi.org/10.1016/j.seppur.2006.08.003>

*Separation and Purification Technology*, 53, 3, pp. 301-311, 2007

#### **NRC Publications Record / Notice d'Archives des publications de CNRC:**

<https://nrc-publications.canada.ca/eng/view/object/?id=a4957ced-96b7-446c-891e-379ea9a2834>

<https://publications-cnrc.canada.ca/fra/voir/objet/?id=a4957ced-96b7-446c-891e-379ea9a28341>

Access and use of this website and the material on it are subject to the Terms and Conditions set forth at

<https://nrc-publications.canada.ca/eng/copyright>

READ THESE TERMS AND CONDITIONS CAREFULLY BEFORE USING THIS WEBSITE.

L'accès à ce site Web et l'utilisation de son contenu sont assujettis aux conditions présentées dans le site

<https://publications-cnrc.canada.ca/fra/droits>

LISEZ CES CONDITIONS ATTENTIVEMENT AVANT D'UTILISER CE SITE WEB.

**Questions?** Contact the NRC Publications Archive team at

PublicationsArchive-ArchivesPublications@nrc-cnrc.gc.ca. If you wish to email the authors directly, please see the first page of the publication for their contact information.

**Vous avez des questions?** Nous pouvons vous aider. Pour communiquer directement avec un auteur, consultez la première page de la revue dans laquelle son article a été publié afin de trouver ses coordonnées. Si vous n'arrivez pas à les repérer, communiquez avec nous à PublicationsArchive-ArchivesPublications@nrc-cnrc.gc.ca.



# Performance of PEI/BMI semi-IPN membranes for separations of various binary gaseous mixtures<sup>☆</sup>

Jamal Kurdi, Ashwani Kumar\*

*Institute for Chemical Process and Environmental Technology, National Research Council of Canada,  
M-12 Montreal Road Campus, Ottawa, Ont. K1A 0R6, Canada*

Received 16 February 2006; received in revised form 28 July 2006; accepted 7 August 2006

## Abstract

Synthesis of polyetherimide–bismaleimide (PEI–BMI) semi-interpenetrating polymer networks (semi-IPNs) combined with solvent phase inversion was used to prepare asymmetric flat membranes, which were coated with silicon rubber. These membranes were evaluated for production of O<sub>2</sub>-enriched air and separation of CO<sub>2</sub> from its mixture with CH<sub>4</sub> as well as with N<sub>2</sub>. Using different preparation schemes membranes with varying skin and supported layer characteristics were prepared. These different morphologies of membranes were responsible for a trade-off performance between gas permeance and permselectivity. These new composite, PEI–BMI semi-IPN membranes showed suitable performance for production of O<sub>2</sub>-enriched air and separation of CO<sub>2</sub> from natural gas or flue gas relevant to greenhouse gas emission control. Membrane performance was explained in terms of the intrinsic gas transport properties of the coated silicon layer and membrane glassy material, which determine the limitations of permeance–permselectivity trade-off. It was also found that the permselectivity for CO<sub>2</sub> over CH<sub>4</sub> or N<sub>2</sub> increases with increasing CO<sub>2</sub> feed concentration. This might be exploited to arrange for more cost-efficient multistage gas separation systems.

Crown Copyright © 2006 Published by Elsevier B.V. All rights reserved.

**Keywords:** Semi-IPN; BMI; PEI; Gas separation membranes

## 1. Introduction

There has been significant growth in the production of natural gas as an efficient and environmentally clean fuel supply [1]. Membrane-based gaseous separation is a green technology that has the potential to improve the economics of natural gas upgrading as well as separation of green house gases (GHG) from flue gases [2]. However, there are challenges in preparing membranes with the desirable combination of high selectivity and high permeability that could achieve competitive gas separation processes in all applications of natural gas industry [3]. The chemical and physical resistance as well as the stability and durability of the developed membranes are also desirable [4].

Novel tailored materials with tuned superior properties and characteristics for gaseous separations could be made by combining soft and hard block phases dispersed at a molecular or nanoscale [5]. For example, a mixed matrix membrane compris-

ing a mixture of a glycol plasticizer, a particulate solid support and silicon rubber coated on a porous support media was discovered to have an improved stability and performance for the separation of gases and processing natural gas [6]. Coating highly porous polysulfone with a composite of silicon rubber and polyethylene glycol produces membranes with a greater selectivity for polar gas (H<sub>2</sub>S) over non-polar gases (methane, carbon dioxide and hydrogen) than that for polysulfone membranes coated with only silicon rubber [7]. The dispersion of nonporous fumed silica nanoparticles into glassy amorphous poly (4-methyl-2-pentyne) produces a reverse-selective membrane by enhancing both the permeability and selectivity of the larger *n*-butane molecules over the smaller methane molecules [8]. An improved alloy-type membrane exhibiting good mechanical strength and desirable hydrophilic membrane properties was prepared from a casting solution of a compatible blend of a vinylidene fluoride polymer and a vinyl acetate polymer that can be hydrolyzed after casting to render hydrophilic surface [9]. However, tailoring useful nanocomposite polymeric membrane still faced with many challenges such as the formation of micro-scale defects, inadequate particle dispersion and poor polymer–particle interfacial adhesion [5,8]. Chemical and phys-

<sup>☆</sup> NRCC No.:49103

\* Corresponding author. Tel.: +1 613 998 0498.

E-mail address: [ashwani.kumar@nrc-cnrc.gc.ca](mailto:ashwani.kumar@nrc-cnrc.gc.ca) (A. Kumar).

Table 1  
Chemical structure of PEI, BMI and NMP

Component	Chemical structure
PEI	
BMI	
NMP	

ical stability of the nanocomposite materials as well as their resistance to plasticization and loss of selectivity due to CO<sub>2</sub> and C<sub>3</sub> + hydrocarbons are important issues that should be considered [10].

Thermoplastic (PEI) and thermosetting (BMI) materials were chosen for their high performance characteristics and commercial availability. We found that *in situ* polymerization of BMI monomer inside PEI/NMP solution forms hard phase of thermoset BMI resin that interpenetrates soft phase of thermoplastic PEI networks, i.e. formation of physical interlock between the two phases. The chemical structures of the semi-interpenetrating polymer network of BMI–PEI have been analyzed by ATR–FTIR and XPS spectroscopy including the description of possible reactions as reported in our earlier work [11]. The BMI–PEI semi-IPN was found to be suitable for gaseous separations [13]. However, these new membranes were not investigated for natural gas, landfill leachate gas, O<sub>2</sub>-enriched air and GHG separation applications. The present work reports use of these materials in formation and characterization of new membranes that are suitable for gaseous mixtures that simulate natural gas and flue gases.

## 2. Experimental

### 2.1. Materials

Aromatic polyetherimide (PEI) Ultem<sup>®</sup> 1000 was supplied by General Electric Plastics, USA in pellet form and was dried in an oven at 150 °C for 8 h before use to remove any possible absorbed water vapors. Anhydrous 1-methyl-2-pyrrolidinone (NMP), Aldrich, 99.5%, reagent grade (water <0.005%) and 1,1'-(methylenedi-4,1-phenylene) bismaleimide (BMI) 95% were supplied by Sigma–Aldrich Canada Ltd. Chemical structures of PEI, BMI and NMP are given in Table 1. Anhydrous ethyl alcohol was received from Commercial Alcohols Inc., Ont., Canada. Hexanes of ACS reagent grade were supplied by VWR, Canada. All solvents were used as supplied under a dry nitrogen atmosphere. Ultra high purity helium, medical air, CO<sub>2</sub> and CH<sub>4</sub> were supplied by BOC Gases Canada Ltd. and were used as received without further purification.

### 2.2. Membrane preparation

Casting solutions with various compositions listed in Table 2 were prepared. PEI was completely dissolved in NMP solvent by rolling the bottle of each sample slowly then, anhydrous EtOH was added with slow mixing until a homogenous solution was obtained. It was possible to reduce the required time for this process by increasing temperature to 60 °C. BMI powder was added to some of these casting solutions (see Table 2) and slow mixing was carried out for one group of samples at ambient condition. A second group of samples was rolled inside a cabinet that was fitted with three infra-red lamps (375 W) with adjustable intensity to control the temperature. In our experiments, it was maintained at 60 °C. The change in color of each sample was monitored and all solutions were cast at different mixing times. Membranes were cast at room temperature on clean glass plates placed in a glove box equipped with a gas filter. After casting each sample with a doctor knife having a gap of 250 μm, the plate was quickly immersed in distilled water at ambient temperature. The membrane films were left in water for 3 days then washed and stored in anhydrous EtOH bath for 1 day. Membranes were subsequently placed in hexanes for 1 day before leaving them in a fume hood for 1 day. Drying was carried out at 80 °C in air-purging convection oven for 1 day and finally in vacuum oven at 80 °C and 96.7 kPa (725 mmHg) for 2 days. Three circular

Table 2  
Compositions of polymeric solutions used in this study

Sample number	Composition, percent (w/w) of the total solution			
	PEI	BMI	NMP	EtOH
1	25	0	62.35	12.65
2	24.75	0.25	62.35	12.65
3	23.75	1.25	62.35	12.65
4	22.5	2.5	62.35	12.65
5	29	0	60	11
6	28.71	0.29	60	11
7	27.55	1.45	60	11
8	26.1	2.9	60	11
9	19.5	0	67.2	13.3
10	17.6	1.9	67.2	13.3

coupons of  $7.4 \times 10^{-2}$  m diameter were cut from each sample to be used in the permeation test while other pieces were cut from the same sample for SEM characterization.

Membranes used in the permeation test were coated with silicon rubber. A solution of 3% Sylgard 184 with a catalyst to base rubber ratio of 1:10 in *n*-pentane was sprayed as a thin layer on the top surface of the membrane and the solvent was allowed to evaporate. Application of four coatings was found to be adequate for making gas separation membranes. Finally, the silicon coated membranes were cured in air purging convection oven at 80 °C for 1 day.

### 2.3. Membrane morphology

Membrane samples without silicon rubber coating were examined by scanning electron microscope (SEM) using JEOL 840A equipment at an accelerating voltage of 10 kV. Samples were prepared by cutting a strip from membrane, freezing in liquid nitrogen and fracturing to obtain a representative sample. They were mounted on carbon tape on 45° SEM stubs and sputter coated with gold. Photographs were taken at different magnifications.

### 2.4. Permeation test

A cross-flow test cell having a permeation surface area of 9.6 cm<sup>2</sup> was used. Pure O<sub>2</sub>, N<sub>2</sub> and medical air were used to study O<sub>2</sub>/N<sub>2</sub> separation. Pure CH<sub>4</sub>, CO<sub>2</sub>, N<sub>2</sub> and their mixture were used to study CO<sub>2</sub>/CH<sub>4</sub> and CO<sub>2</sub>/N<sub>2</sub> separations. Feed pressure of 665 kPa gauge (498.8 cmHg) was used and the retentate was set at a flow rate of  $6.6 \times 10^{-6}$  m<sup>3</sup>(STP) s<sup>-1</sup> while permeate was discharged to atmosphere. The permeate flow rate was measured by a soap bubble flow meter and O<sub>2</sub>, CH<sub>4</sub> and CO<sub>2</sub> concentrations of feed and permeate gas mixtures were determined by gas chromatography.

## 3. Results and discussion

Synthesis procedure for PEI–BMI semi-IPNs combined with membrane formation was finalized after several preliminary experiments. It was observed that BMI could be polymerized slowly inside and through PEI/NMP solutions at ambient conditions in the presence of ethyl alcohol [11–13]. The progress of polymerization was followed by measuring the viscosity, color change and spectroscopic analysis as discussed in details in our earlier work [11]. It is worth noting that *in situ* anionic polymerization of BMI has many advantages such as avoiding the addition of complicated initiators or catalysts as well as obtaining low molecular weight thermosetting polymer as discussed elsewhere [14]. Using EtOH as a proton donor, the color of the PEI–BMI polymeric solution underwent gradual change from light yellow to bright crimson. It was worth noting that the polymerization rate of BMI depends on the transparency of the used bottle, the speed of mixing, the intensity of light, temperature, composition and concentration of the polymer solution. Absorption of water vapor during preparation of the solution

might also have an influence on the rate of BMI polymerization. For our samples we observed that at room temperature, the solution need from 11–24 days for onset of color change while at 60 °C, color changed in less than 24 h. It was observed that color change was faster for transparent bottles, more intense light, lower BMI concentration, lower viscosity and higher speed of mixing. Appearance of dark red color was an indication for complete polymerization of BMI to a low molecular weight resin and mixing for longer time did not lead to a significant change in the solution. This was due to anionic polymerization of BMI that usually led to a low molecular weight polymer as discussed elsewhere [14]. All polymer solutions were suitable for producing gas separation membranes as long as there is no large phase separation or precipitation. It was worth noting that the samples mixed at 60 °C, BMI had significantly shorter polymerization time than those samples mixed at room temperature. Regardless of mixing temperatures ripe solutions, as indicated by red color, of same compositions formed membranes with no significant differences in their morphology or separation performance.

### 3.1. Morphology analysis

Membrane morphology plays an important role in determining membrane performance for gas separations. Therefore, membranes were examined by scanning electron microscopy (SEM) to show the change in the morphology that might influence the performance of gas separation membranes. As shown in Fig. 1, membranes labeled (a) that was produced from casting solution containing 19.5 wt.% polymer have an apparent thickness of 148 μm and membranes labeled (b) that was made from a solution containing 29 wt.% polymer had an apparent thickness of 170.5 μm. This means that the shrinkage of membrane (a) due to coagulation is higher, which led to a thinner structure and larger number of fingers (see Fig. 1) than those in membrane (b). For quantitative comparison of the differences between these two membranes (a and b), additional measurements and calculations were done. The weights of these dried membranes (a and b) of 16 cm<sup>2</sup> area were determined by a balance (least count 0.0001 g). The density of two polymer solutions used to produce the above mentioned membranes (a and b) were determined using the same balance and 100 ml volumetric flasks with class A glass stopper. For an area of 16 cm<sup>2</sup>, the weight of the used solution was calculated from the corresponding polymer concentration and the net polymer weight. The volume of the solution was calculated from its weight and density. The thickness of the solution was calculated from its volume and area (i.e. 16 cm<sup>2</sup>). The apparent density of the two membranes was calculated by divided membrane weight by its apparent volume. The results are shown in Table 3. It was clear that the apparent density of membrane (a) was lower than that for membrane (b) by 26% and the total thickness was reduced by 13%. Although we used same doctor blade (i.e. gap of 250 μm), the thickness of membrane cast with solution (b) has to be 262 μm in order to produce 16 cm<sup>2</sup> dried membrane that weighs 0.1227 g. This means that a slight swelling of the more viscous solution (b) took place during casting process that was similar to die swelling as illustrated elsewhere [15]. According to Ismail and Hassan [16] shear

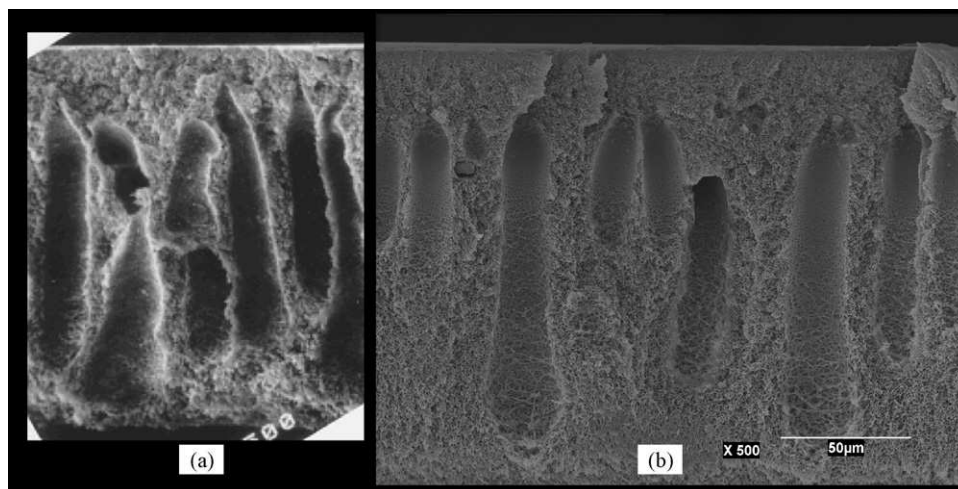


Fig. 1. Morphologies of membranes produced from casting solutions containing 19.5% polymer concentration (a) and 29% polymer concentration (b). SEM was obtained at the same magnification 500 $\times$  and the same scale distance was used for both membranes.

rate is a function of the velocity of casting knife and membrane thickness. Therefore, the shear rate that influences membrane morphology and performance as discussed elsewhere [15,17] was not the same for the two membranes when the same speed of casting knife is used. It is worth noting that the skin layer thickness of the two membranes was comparable.

Spongy structure of these membranes might also be influenced by solution compositions and gellation conditions as discussed elsewhere [18]. Fig. 2 shows the top and bottom parts of the cross-sections of membranes (a) and (b). It is clear that the cross-section of the top skin layer membrane (a) has higher porosity than membrane (b). Also the cross-section of bottom spongy layer has a higher porosity than the top skin layer for both membranes. This increase in the spongy pore size especially for the bottom layer could be attributed to increased amount of solvent (NMP) in the coagulation medium (water). A similar phenomenon was also reported elsewhere [19].

Regardless of the membrane materials, the above morphology observations indicate that membrane preparation procedures play an important role in determination of the size, shape and distribution of pore or free volume. Generally, solution containing high polymer concentration (usually more than 25% (w/w) of polymer) might produce membranes with a tighter structure and lower free volume compared to the membranes produced

from solutions containing a lower polymer concentration (e.g. 19.5%). The tighter morphology leads to membranes with a low fluid flux and high interactions between the transported fluid and the membrane materials that might lead to an improved fluid permselectivity. The less tight morphology leads to an opposite influence on the fluid flux and permselectivity. Therefore, various membranes could be produced from the same materials that have varying morphology with a trade-off between membrane permeance and permselectivity. This trade-off, which is related to membrane morphology resulted from using different preparation method, is different from the Robeson's trade-off [20] that is used to compare different membrane materials but not different membrane morphology. The ability to tailor these membranes and control their morphology has been reported elsewhere [21,22].

### 3.2. Gas transport characteristics

#### 3.2.1. Air separation

Semi-IPN PEI–BMI membranes were evaluated for permeation of pure oxygen and nitrogen as well as for air. Fig. 3 shows the trade-off curve plot of O<sub>2</sub>/N<sub>2</sub> permselectivity versus O<sub>2</sub> permeance based on permeation of pure gases. As we have discussed in the morphology analysis section, it is

Table 3  
Apparent volume<sup>a</sup> and thickness of two membranes (a and b) as well as for their corresponding solutions with 19.5% and 29% (w/w) polymers, respectively

Sample	Area (cm <sup>2</sup> )	Polymer concentration (%)	Polymer weight <sup>a</sup> (g)	Solution density (g/cm <sup>3</sup> )	Thickness (cm)	Apparent volume <sup>a</sup> (cm <sup>3</sup> )	Apparent density (g/cm <sup>3</sup> )
Solution (a)	16	19.5	0.0785	1.0066 <sup>b</sup>	0.02500 <sup>c</sup>	0.3999	–
Solution (b)	16	29	0.1227	1.0100 <sup>b</sup>	0.02618 <sup>c</sup>	0.4189	–
Membranes (a)	16	–	0.0785	–	0.01480 <sup>d</sup>	0.2368	0.3315
Membranes (b)	16	–	0.1227	–	0.01705 <sup>d</sup>	0.2728	0.4498

<sup>a</sup> Corresponding to 16 cm<sup>2</sup> area.

<sup>b</sup> Measured.

<sup>c</sup> Calculated.

<sup>d</sup> Measured by SEM.

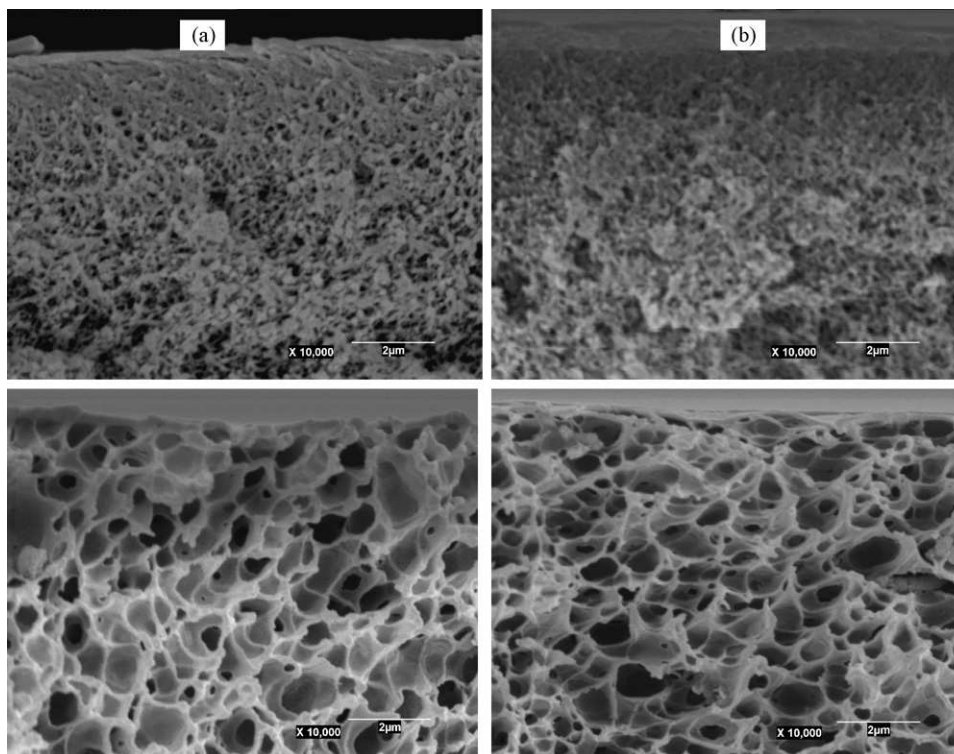


Fig. 2. Cross-section SEM of membranes produced from casting solutions containing 19.5% polymer concentration (a) and 29% polymer concentration (b). Top two photographs represent the top layer of each membrane and the two bottom photographs represent the bottom layer of each membrane.

possible to control membrane morphology and its apparent density through changing the preparation procedures. Although Fig. 3 shows the decrease in the  $O_2/N_2$  permselectivity with an increase in the  $O_2$  permeance, the rate of these changes is not constant and might be divided into two regions. The first region represent permeance ranging up to 30 GPU (the gas permeation unit, GPU =  $10^{-6} \text{ cm}^3(\text{STP})/(\text{cm}^2 \text{ s cmHg})$  or  $3.35 \times 10^{-10} \text{ mol}/(\text{m}^2 \text{ s Pa})$  in SI unit) where there is a steep decrease in the  $O_2/N_2$  permselectivity with a slight increase

in the  $O_2$  permeance. In this region, the dominant interactions are between the permeable gases and the semi-IPN PEI–BMI networks. The improvement in the  $O_2/N_2$  permselectivity might be attributed to membrane skin integrity that could be explained by the polymer chain orientation and gradual change in the microscopic porosity through the cross-section of the membrane skin. As there is a slight change in the gas permeance, it is possible that the denser of the top surface of the skin layer is accompanied with a less dense structure for the rest of the skin (transition layer) and vice versa. For example we were not able to make PEI membranes with  $O_2/N_2$  permselectivity equal or greater than 7, it was possible to make semi-IPN PEI–BMI membranes with  $O_2/N_2$  permselectivity of slightly larger than 7. This indicates that the new membrane material has a superior ability to form improved membrane skin integrity compared to using PEI alone as a membrane material. Therefore, both procedures for membrane preparation in addition to membrane material characteristics are of great importance for improving performance of gas separation membranes. The influence of shear rate on the morphology and separation performance of hollow fiber membranes was first studied by Chung et al [23]. Recently, Ismail and Hassan [16] reported the preparation of asymmetric polysulfone nanofiltration flat membranes, and showed that decreasing the polymer concentration or increasing the shear rate (up to a critical shear rate) led to an increase in the pure water permeation but a decrease in the percentage of salt rejection. A similar observation on the influence of shear rate in membrane preparation on the membrane performance for  $\text{CO}_2/\text{CH}_4$  separation was reported elsewhere [17].

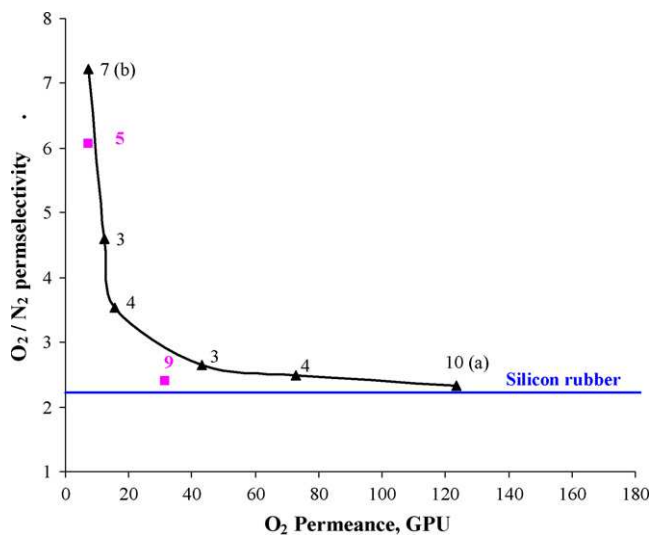


Fig. 3. Trade-off curve plot of  $O_2$  permeance and  $O_2/N_2$  permselectivity based on the permeation of pure gases. Filled square symbols are for PEI membranes without BMI. Labels correspond to the sample number listed in Table 2.

In the second region (permeance higher than 30 GPU), there is a slight decrease in the  $O_2/N_2$  permselectivity with the increase in the  $O_2$  permeance. This permselectivity is close to the intrinsic  $O_2/N_2$  permselectivity for silicon rubber (i.e.  $\alpha = 2.22$ ) that was coated on the membrane. It is clear that the interactions between the permeable gases and the coated silicon rubber in this region are dominant. The large increase in the gas permeance was attributed to the decrease in the gas transport resistance of the supported layer (i.e. semi-IPN PEI–BMI membrane). However, there is a limitation on the increase of gas permeance by an increase in the free volume of the supported layer that might lead to a decrease in its mechanical strength or creation of large defects. As reported by Koros et al. [15], these defects should be small enough in order to have the ability to caulk the membrane skin with silicon rubber and eliminate the Knudsen flow through these defects that deteriorate membrane gas permselectivity.

Using air as a feed gas a trade-off curve between  $O_2/N_2$  permselectivity and  $O_2$ -enriched air permeance was observed as shown in Fig. 4. It was worth noting that the semi-IPN PEI–BMI membranes had an improved performance for  $O_2/N_2$  separation compared to PEI membranes without BMI. This might be attributed to an improved membrane skin integrity that led to an increase in  $O_2/N_2$  permselectivity with a slight decrease in gas permeance. It was further observed that membrane labeled (b) in this work had  $O_2$ -enriched air permeance of 9 GPU and  $O_2/N_2$  permselectivity of 7. Conversely, we observed an increase in the gas permeance due to a decrease in the gas transport resistance of the membranes without formation of defects, which are not small enough to be caulked by the silicon rubber. For example membrane labeled (a) in this work has  $O_2$ -enriched air permeance of more than 150 GPU and  $O_2/N_2$  permselectivity of 2.2.

### 3.2.2. $CO_2/CH_4$ separation

Performance of semi-IPN PEI–BMI membranes were studied through the permeation of  $CO_2$ ,  $CH_4$  and their mixtures. The

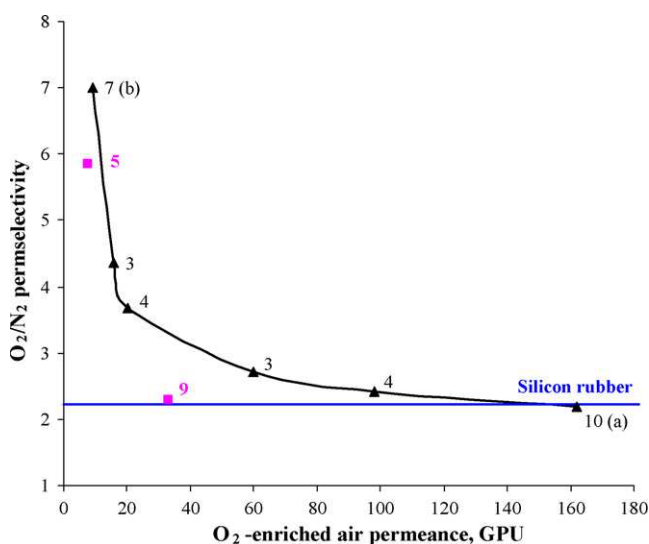


Fig. 4. Trade-off curve plot of  $O_2$ -enriched air permeance and  $O_2/N_2$  permselectivity based on the permeation of air. Filled square symbols are for PEI membranes without BMI. Labels correspond to the sample number listed in Table 2.

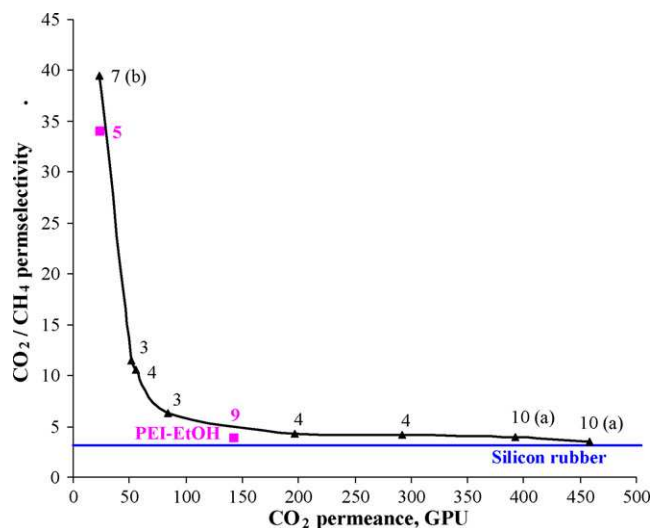


Fig. 5. Trade-off curve plot of  $CO_2$  permeance and  $CO_2/CH_4$  permselectivity based on the permeation of pure gases. Filled square symbols are for PEI membranes without BMI. Labels correspond to the sample number listed in Table 2.

trade-off curve of  $CO_2$  permeance and  $CO_2/CH_4$  permselectivity based on permeation of pure gases is shown in Fig. 5. On one hand it was possible to have a membrane with  $CO_2$  permeance of 23.3 GPU and ideal  $CO_2/CH_4$  permselectivity of 39.5. On the other hand, a membrane with  $CO_2$  permeance of 458 GPU and ideal  $CO_2/CH_4$  permselectivity of 3.5 was also obtained. There is a slight improvement in the performance of semi-IPN PEI–BMI membranes over PEI membranes without BMI (see Fig. 5). The permeation test for pure  $CH_4$  was carried out before using pure  $CO_2$  permeation test. It is worth noting that repeating the pure  $CH_4$  permeation test immediately after using  $CO_2$  produced the same results indicating that there were no  $CO_2$  plasticization or dilation effects [24] on these membranes.

From permeation data of  $CO_2$  and  $CH_4$  mixtures, shown in Fig. 6, it is clear that the observed gas permeance and  $CO_2/CH_4$  permselectivity are lower than those determined by pure gas permeation test shown in Fig. 5. We were able to form a membrane with gas permeance of 6.3 GPU and  $CO_2/CH_4$  permselectivity of 18.3 as well as another membrane with gas permeance of 286 GPU and  $CO_2/CH_4$  permselectivity of 2.6. Fig. 6 shows a significant improvement in the performance of semi-IPN PEI–BMI membranes over PEI membranes without BMI for gas mixtures.

### 3.2.3. Case study for $CO_2/CH_4$ separation using four semi-IPN PEI–BMI membranes

Four semi-IPN PEI–BMI membranes:  $s_2$ ,  $s_3$ ,  $s_4$  and  $s_{10}$  were selected for further studies. The subscript indicates the sample numbers shown in Table 2. The impact of pure  $CO_2$  feed pressure on the plasticization of these membranes and the effects of  $CO_2$  concentration of the feed gas mixtures on the membrane performance were investigated. Pure  $CO_2$  permeances through these four membranes at different feed pressure are shown in Fig. 7. It is clear that there was no change in the  $CO_2$  permeance up to pressures of 1400 kPa for all four membranes. Therefore, one could conclude that the increase in the pressure up to 1400 kPa

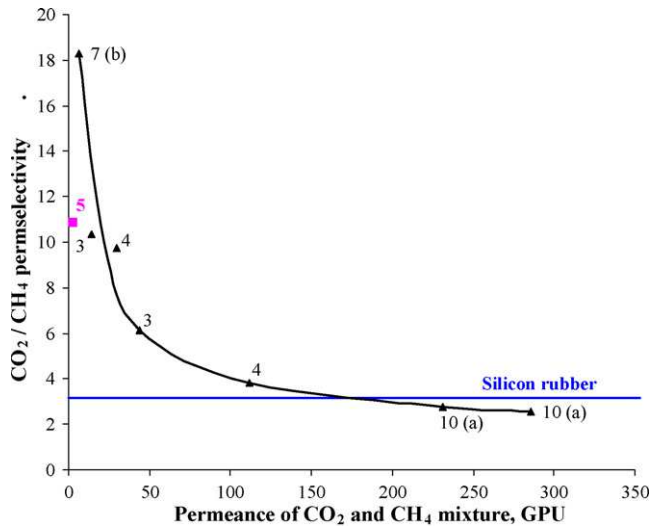


Fig. 6. Trade-off curve plot of permeance of the mixture of CO<sub>2</sub> and CH<sub>4</sub> vs. CO<sub>2</sub>/CH<sub>4</sub> permselectivity based on the permeation of gas mixture containing 26.5% (v/v) CO<sub>2</sub> and 73.5% (v/v) CH<sub>4</sub>. Filled square symbols are for PEI membranes without BMI. Labels correspond to the sample number listed in Table 2.

did not plasticize these membranes according to the literature reported [25] definition of plasticization. These results are different from plasticization of thin-film glassy polymers that has been reported and discussed elsewhere [26]. However, when a mixture of CO<sub>2</sub> and CH<sub>4</sub> is used, the gas permeance decreases slightly with the increase in the CO<sub>2</sub> concentrations in the feed gas mixture as shown in Fig. 8. The decrease in the CO<sub>2</sub> permeance by increasing CO<sub>2</sub> concentrations in the feed gas mixture was also observed by others [27–29]. As the feed pressure is constant at 827 kPa (120 psig) the slight decrease in the permeance might be attributed to the CO<sub>2</sub> adsorption coverage as illustrated elsewhere [27].

The driving force for permeating a gas from a mixture through a membrane is usually represented by the difference in the partial pressure of this gas between permeate and feed sides. Fig. 9 shows that with an increase in the CO<sub>2</sub> feed concentration the

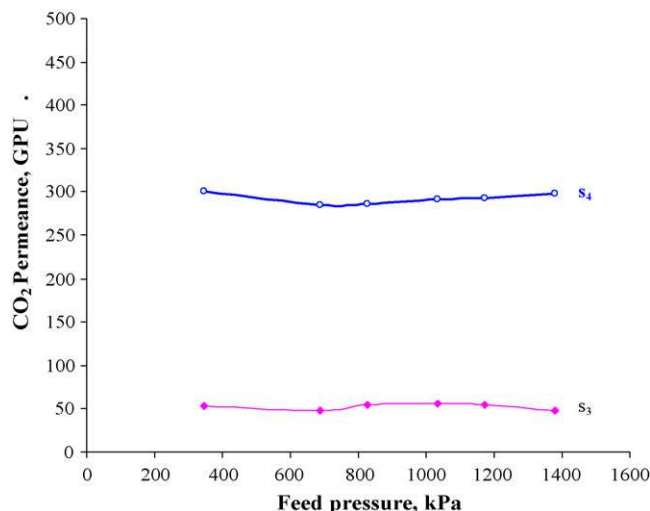


Fig. 7. Permeance of pure CO<sub>2</sub> at different feed pressures for different semi-IPN membranes.

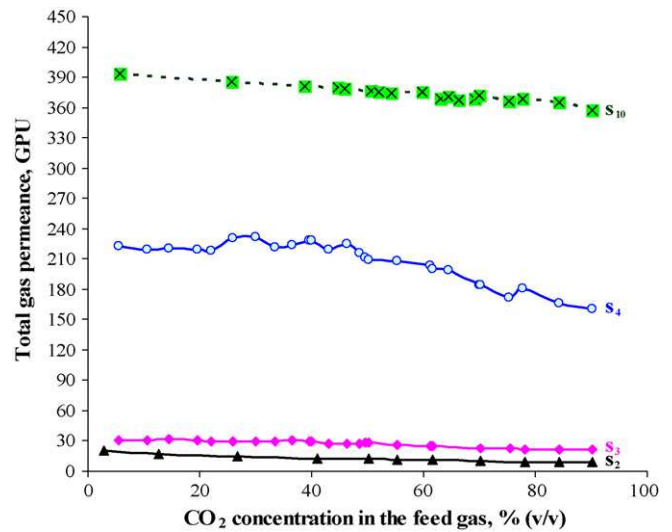


Fig. 8. Total gas permeance of CO<sub>2</sub> and CH<sub>4</sub> mixture at different feed concentrations.

partial pressure differences increases for CO<sub>2</sub> while decreases for CH<sub>4</sub>. All four semi-IPN PEI–BMI membranes have approximately the same linear correlation between the CO<sub>2</sub> feed concentration and the permeation driving force. On one hand, increasing the permeation driving force of CO<sub>2</sub> leads to an increase in the permeation rate of CO<sub>2</sub> and on the other hand, decreasing the permeation driving force of CH<sub>4</sub> leads to a decrease in the permeation rate of CH<sub>4</sub> and therefore improved CO<sub>2</sub>/CH<sub>4</sub> permselectivity. The phenomenon of increasing the productivity of the more permeable gas (i.e. CO<sub>2</sub>) upon increasing its driving force through the membrane was reported by Ismail and Yacob [30], however, they did not refer to the simultaneous change in the driving force of other gases in the mixture. It is worth noting that the driving forces for CO<sub>2</sub> and CH<sub>4</sub> become equal when the concentration in the feed mixture is around 55% (v/v) of CO<sub>2</sub> gas. Therefore, a 50% concentration of each gas in a binary mixture does not necessarily lead to equal driving forces

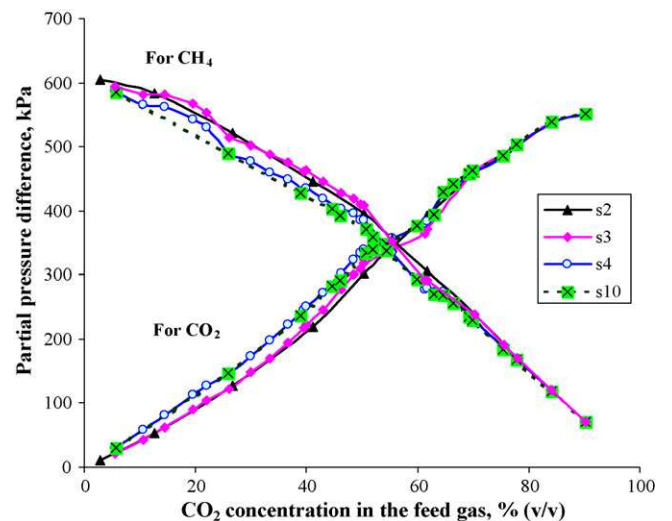


Fig. 9. Partial pressure differences (driving force) for CO<sub>2</sub> and CH<sub>4</sub> at different feed concentrations.

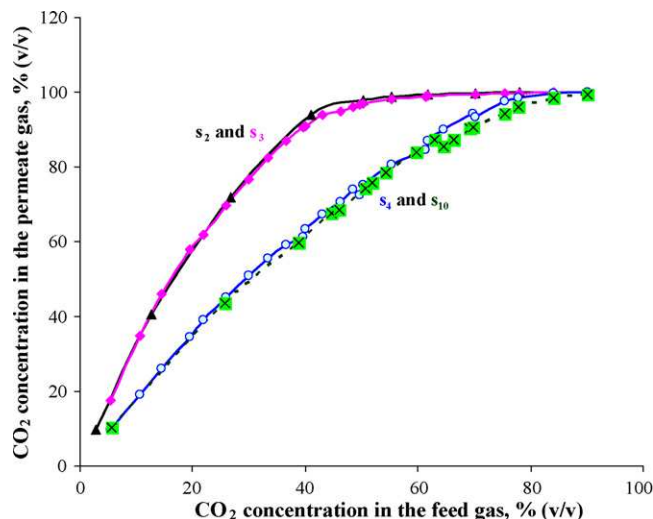


Fig. 10. CO<sub>2</sub> concentration of permeate gas mixture of CO<sub>2</sub> and CH<sub>4</sub> at different feed concentrations.

for both gases. Also at CO<sub>2</sub> feed concentration lower than 20% (v/v), the higher driving force for CH<sub>4</sub> than that for CO<sub>2</sub> might lead to CH<sub>4</sub> flux that is higher than CO<sub>2</sub> flux through the membrane. This was due to a CO<sub>2</sub> permeate concentration of lower than 50%. In all cases, the CO<sub>2</sub> permeance is always greater than CH<sub>4</sub> permeance and the CO<sub>2</sub> concentration in permeate is always higher than that in the feed.

The influence of CO<sub>2</sub> feed concentration in CO<sub>2</sub> and CH<sub>4</sub> mixture on the permeate composition is illustrated in Fig. 10. With increasing CO<sub>2</sub> feed concentration, the rate of increase of CO<sub>2</sub> concentration in the permeate is higher for s<sub>2</sub> and s<sub>3</sub> membranes and their curves show a plateau at CO<sub>2</sub> feed concentration of greater than 40% (v/v) compared to s<sub>4</sub> and s<sub>10</sub> membranes that have lower rate and their curves show a plateau at CO<sub>2</sub> feed concentration of greater than 80% (v/v). This plateau in curves means that the partial pressure of gases in the permeate side becomes approximately constant while there is still room to increase the partial pressure of CO<sub>2</sub> and decrease the partial pressure of CH<sub>4</sub> on the feed side. For this reason and as shown in Fig. 9, there is no observed plateau for the partial pressure differences of CH<sub>4</sub> while the plateau for CO<sub>2</sub> appears at CO<sub>2</sub> feed concentration that is higher than 85% (v/v). The plateau for CH<sub>4</sub>, shown in Fig. 9, appears at CO<sub>2</sub> feed concentrations of lower than 15% (v/v).

The influence of CO<sub>2</sub> feed concentration on CO<sub>2</sub>/CH<sub>4</sub> permselectivity for a mixture is illustrated in Fig. 11. It is clear that the CO<sub>2</sub>/CH<sub>4</sub> permselectivity starts to increase significantly at CO<sub>2</sub> feed concentration of greater than 40% (v/v) for s<sub>2</sub> and s<sub>3</sub> membranes and at concentration of greater than 80% (v/v) for s<sub>4</sub> and s<sub>10</sub> membranes. These concentrations are the same where the plateau starts as shown in Fig. 10. The increase in the CO<sub>2</sub>/CH<sub>4</sub> permselectivity is attributed to the increase in the permeation driving force of CO<sub>2</sub> and the decrease in the driving force of CH<sub>4</sub> through the membranes. The phenomenon of increasing the permselectivity upon increasing the concentration of more permeable gas (i.e. CO<sub>2</sub>) in the feed was also observed and discussed elsewhere [31,32].

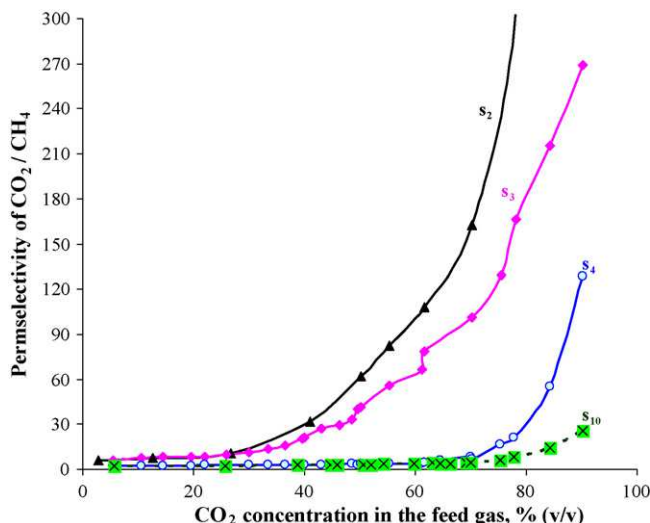


Fig. 11. Permselectivity of CO<sub>2</sub> over CH<sub>4</sub> at different CO<sub>2</sub> feed concentrations.

The CO<sub>2</sub>/CH<sub>4</sub> permselectivity and permeance of CO<sub>2</sub> and CH<sub>4</sub> mixture was plotted in Fig. 12. Larger symbols represent the values that are determined from permeation of corresponding pure gases. For s<sub>2</sub> and s<sub>3</sub> membranes, there was no significant change in the gas permeance while the CO<sub>2</sub>/CH<sub>4</sub> permselectivity increased with increasing CO<sub>2</sub> feed concentration. Permeation data of pure gases show a higher permeance and CO<sub>2</sub>/CH<sub>4</sub> permselectivity than those observed for CO<sub>2</sub> and CH<sub>4</sub> mixture at lower CO<sub>2</sub> feed concentrations (less than 40% (v/v)). For s<sub>4</sub> and s<sub>10</sub> membranes, the gas permeance decreases with increasing CO<sub>2</sub> feed concentration and then becomes constant. Permeation data of pure gases show greater permeance than those observed for CO<sub>2</sub> and CH<sub>4</sub> mixture with a difference greater than that for s<sub>2</sub> and s<sub>3</sub> membranes. The CO<sub>2</sub>/CH<sub>4</sub> permselectivity starts to increase significantly at a higher CO<sub>2</sub> feed concentration for s<sub>4</sub> and s<sub>10</sub> membranes compared to s<sub>2</sub> and s<sub>3</sub> membranes. These results confirm that the change in CO<sub>2</sub> feed concentration has greater influence on the CO<sub>2</sub>/CH<sub>4</sub> permselectivity for s<sub>2</sub> and s<sub>3</sub>

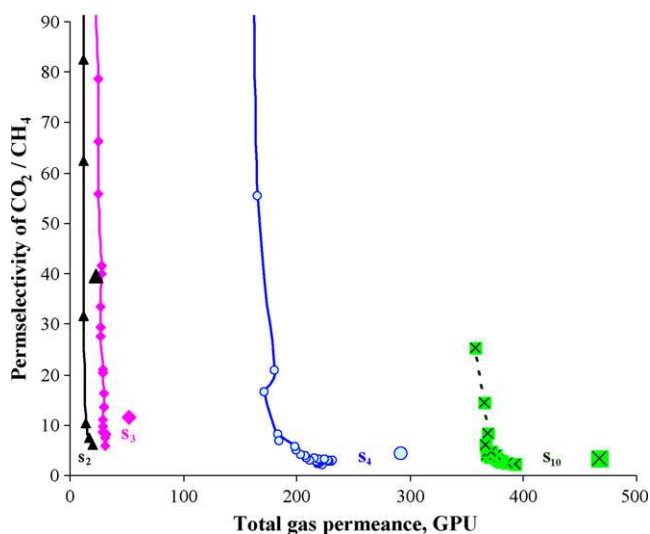


Fig. 12. Permselectivity of CO<sub>2</sub> over CH<sub>4</sub> vs. gas permeance at different CO<sub>2</sub> feed concentrations.

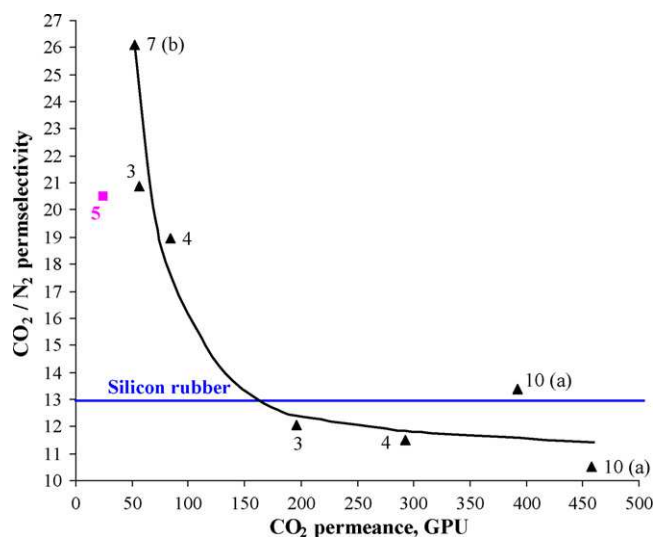


Fig. 13. Trade-off curve plot of  $\text{CO}_2$  permeance and  $\text{CO}_2/\text{N}_2$  permselectivity based on the permeation of pure gases. Filled square symbol is for PEI membranes without BMI. Labels correspond to the sample number listed in Table 2.

membranes than those for  $s_4$  and  $s_{10}$  membranes while it has a greater influence on the gas permeance for  $s_4$  and  $s_{10}$  membranes than those for  $s_2$  and  $s_3$  membranes. Dhingra [28] reported that the change in  $\text{CO}_2$  feed concentration in  $\text{CO}_2$  and  $\text{CH}_4$  mixture has an influence on gas transport characteristics for glassy polymers but not for rubbery polymers. Although performance of  $s_4$  and  $s_{10}$  membranes is controlled by the gas transport characteristics of silicon rubber, the performance of these membranes is not independent of  $\text{CO}_2$  feed concentration as reported by Dhingra [28]. It appears that the behavior of silicon rubber as an ultra-thin film or when it is inside a confined space (nanoscale free volume in the glassy polymer) is different from the behavior of thick film of silicon rubber.

### 3.2.4. $\text{CO}_2/\text{N}_2$ separation

The trade-off curve of  $\text{CO}_2$  permeance versus  $\text{CO}_2/\text{N}_2$  permselectivity based on permeation of pure gases is shown in Fig. 13. The observations in Fig. 13 are similar to that found in Fig. 5 for  $\text{CO}_2/\text{CH}_4$  separation. By selecting suitable membrane preparation procedures and conditions, it is possible to have a semi-IPN PEI–BMI membrane with  $\text{CO}_2$  permeance of 52 GPU and  $\text{CO}_2/\text{N}_2$  ideal permselectivity of 26 or a membrane with  $\text{CO}_2$  permeance of 392.7 GPU and  $\text{CO}_2/\text{N}_2$  ideal permselectivity of 13.4. It is clear that there is a significant increase in gas permeance through semi-IPN PEI–BMI membranes compared to PEI membrane without BMI. The silicon rubber shows an ideal  $\text{CO}_2/\text{N}_2$  permselectivity of 13.0 as found elsewhere [20]. Therefore decreasing the gas transport resistance of the supported membrane and avoiding large defects could greatly improve the membrane productivity at this  $\text{CO}_2/\text{N}_2$  permselectivity for silicon rubber.

Fig. 14 shows the influence of  $\text{CO}_2$  feed concentration in  $\text{CO}_2$  and  $\text{N}_2$  mixture on the  $\text{CO}_2/\text{N}_2$  permselectivity for  $s_3$  and  $s_4$  membranes. It is clear that the  $\text{CO}_2/\text{N}_2$  permselectivity starts to increase significantly at  $\text{CO}_2$  feed concentration of greater than 37% (v/v) for  $s_3$  membrane while a slight increase up to

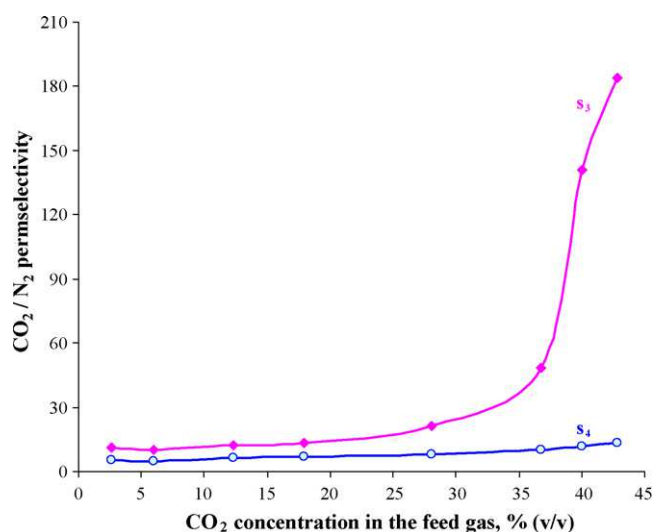


Fig. 14. Permselectivity of  $\text{CO}_2$  over  $\text{N}_2$  at different  $\text{CO}_2$  feed concentrations.

45% for  $s_4$  membrane. The behavior of these two membranes for  $\text{CO}_2/\text{N}_2$  separation is similar for  $\text{CO}_2/\text{CH}_4$  separation as shown in Fig. 11.

The performance of  $s_3$  and  $s_4$  membranes for separation of  $\text{CO}_2$  and  $\text{N}_2$  mixture is shown in Fig. 15. The observations were similar to earlier discussion on  $\text{CO}_2$  and  $\text{CH}_4$  mixtures. However,  $s_4$  membrane does not show a decrease in the gas permeance at low  $\text{CO}_2$  feed concentration when  $\text{CH}_4$  is used instead of  $\text{N}_2$  (see Fig. 12). This might be due to different interactions of  $\text{CH}_4$  with membrane materials or with  $\text{CO}_2$  compared to  $\text{N}_2$  gas. The increase of  $\text{CO}_2/\text{N}_2$  or  $\text{CO}_2/\text{CH}_4$  permselectivity with increasing  $\text{CO}_2$  feed concentration has a great economic benefit as it is possible to arrange the separation process at different stages where the higher permselectivity can be exploited to achieve an improved overall efficiency. The arrangement of separation processes becomes more flexible and efficient with having two types of membranes such as high permeance  $s_4$  and  $s_{10}$  membranes and high permselectivity  $s_2$  and  $s_3$  membranes. It is clear that

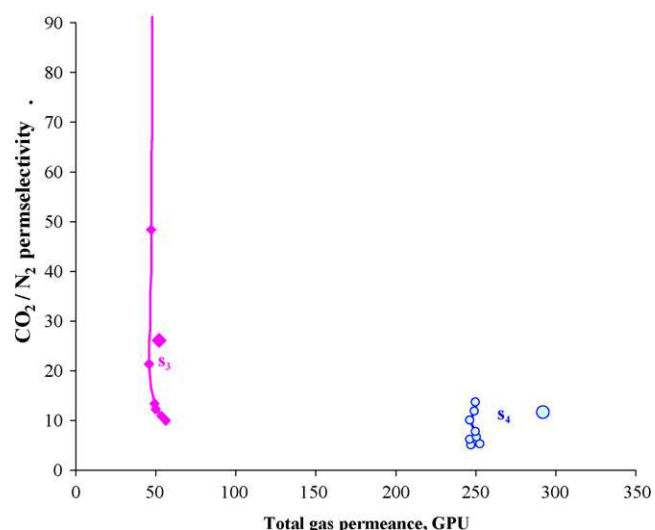


Fig. 15. Permselectivity of  $\text{CO}_2$  over  $\text{N}_2$  versus gas permeance at different  $\text{CO}_2$  feed concentrations.

these membranes made from the novel semi-IPN PEI–BMI show promising results to separate CO<sub>2</sub> from natural gas or flue gas as an important step to control the emission of greenhouse gases.

#### 4. Conclusion

It was possible to prepare semi-IPN PEI–BMI membranes that have a higher performance for gas separations than PEI membranes. Membrane morphology for the skin and the supported layer is greatly influenced by preparation procedures and conditions that usually led to different distributions of the free volume in the produced membranes at scales ranging from molecular dimensions to micrometer. Regardless of membrane materials, changing membrane morphology especially for the skin layer or the supported layer, it was possible to produce membranes with a high gas permeance but a low permselectivity or membranes with a high permselectivity but a low gas permeance. Using cast solution containing 19.5% (w/w) of PEI and BMI polymers, it was possible to decrease significantly the gas transport resistance of the supported membrane layer but it was difficult to obtain improved skin integrity, which is responsible for high permselectivity. On the other hand, using cast solution containing 25% (w/w) or more of PEI and BMI polymers, it is possible to obtain improved skin integrity with a high permselectivity but the supported membrane layer becomes more resistant to gas transport. Using these two types of membranes, one could develop new processes with multiple separation stages to obtain a cost-efficient separation system.

Semi-IPN PEI–BMI membranes were not plasticized by increasing the feed pressure of pure CO<sub>2</sub> up to 1400 kPa. However, CO<sub>2</sub> feed concentration had a significant influence on separation of CO<sub>2</sub> and CH<sub>4</sub> or CO<sub>2</sub> and N<sub>2</sub> mixtures. It was concluded that there would be a slight decrease in the gas permeance with increasing CO<sub>2</sub> feed concentration. The driving force represented by the difference in the partial pressure for each gas in a binary mixture was found to have a nearly linear correlation with CO<sub>2</sub> feed concentration. At low CO<sub>2</sub> feed concentration, the driving force for CH<sub>4</sub> was higher than that for CO<sub>2</sub> but the permeance of CO<sub>2</sub> was higher than the permeance of CH<sub>4</sub>, which always led to a higher CO<sub>2</sub> concentration in the permeate side than that in the feed side.

Using our semi-IPN PEI–BMI membranes, the increase of CO<sub>2</sub>/N<sub>2</sub> or CO<sub>2</sub>/CH<sub>4</sub> permselectivity with increasing CO<sub>2</sub> feed concentration might be economically exploited to arrange more cost-efficient separation systems to capture CO<sub>2</sub> from natural gas or flue gas. It is also possible to use these membranes for production of O<sub>2</sub>-enriched air or separation of various other gases.

#### Acknowledgement

The authors are thankful to Mr. David Kingston for his help with SEM experiments.

#### References

[1] Technical report, Fueling the future: natural gas and new technologies for a cleaner 21st century, Washington Policy and Analysis Inc., Washington, DC, February 2000.

- [2] D. Paul, S.K. Sikdar, Clean Production with Membrane Technology, Clean Products and Processes, vol. 1, Springer-Verlag, New York, 1998, pp. 39–48.
- [3] G.C. Kapantaidakis, G.H. Koops, High flux polyethersulfone–polyimide blend hollow fiber membranes for gas separation, *J. Membr. Sci.* 204 (2002) 153–171.
- [4] W.J. Koros, R. Mahajan, Pushing the limits on possibilities for large scale gas separation: which strategies, *J. Membr. Sci.* 175 (2000) 181–196.
- [5] G. Schmidt, M.M. Malwitz, Properties of polymer–nanoparticle composites, *Curr. Opin. Colloid Interf. Sci.* 8 (2003) 103–108.
- [6] S. Kulprathipanja, J. Charoenphol, Mixed matrix membrane for separation of gases, *US Patent* 6,726,744 (2004).
- [7] S. Kulprathipanja, S.S. Kulkarni, Separation of polar gases from non-polar gases, *US Patent* 4,608,060 (1986).
- [8] T.C. Merkel, B.D. Freeman, R.J. Spontak, Z. He, I. Pinnau, P. Meakin, A.J. Hill, Ultraporous, reverse-selective nanocomposite membranes, *Science* 296 (2002) 519–522.
- [9] S.Z. Jakabhazy, L.J. Zeman, Microporous polymeric membrane, *US Patent* 4,302,334 (1981).
- [10] R.W. Baker, Future directions of membrane gas separation technology, *Ind. Eng. Chem. Res.* 41 (2002) 1393–1411.
- [11] J. Kurdi, A. Kumar, Structuring and characterization of a novel highly microporous PEI/BMI semi-interpenetrating polymer network, *Polymer* 46 (2005) 6910–6922.
- [12] J. Kurdi, A. Kumar, Synthesis and characterization of modified bismaleimide–polysulfone semi-interpenetrating polymer networks, *J. Appl. Polym. Sci.*, in press.
- [13] J. Kurdi, A. Kumar, Formation and thermal stability of BMI-based interpenetrating polymers for gas separation membranes, *J. Membr. Sci.* 280 (2006) 234–244.
- [14] P.O. Tawney, R.H. Snyder, R.P. Conger, K.A. Leibbrand, C.H. Stiteler, A.R. Williams, The chemistry of maleimide and its derivatives. II. Maleimide and *N*-methylolmaleimide, *J. Org. Chem.* 26 (1961) 15–21.
- [15] D.W. Wallace, C. Staudt-Bickel, W.J. Koros, Efficient development of effective hollow fiber membranes for gas separations from novel polymers, *J. Membr. Sci.* 278 (2006) 92–104.
- [16] A.F. Ismail, A.R. Hassan, Formation and characterization of asymmetric nanofiltration membrane: effect of shear rate and polymer concentration, *J. Membr. Sci.* 270 (2006) 57–72.
- [17] J.-J. Qin, T.-S. Chung, C. Cao, R.H. Vora, Effect of temperature on intrinsic permeation properties of 6FDA-durene/1,3-phenylenediamine (mPDA) copolyimide and fabrication of its hollow fiber membranes for CO<sub>2</sub>/CH<sub>4</sub> separation, *J. Membr. Sci.* 250 (2005) 95–103.
- [18] R.-C. Ruaan, T. Chang, D.-M. Wang, Selection criteria for solvent and coagulation medium in view of macrovoid formation in the wet phase inversion process, *J. Polym. Sci. B: Polym. Phys.* 37 (1999) 1495–1502.
- [19] D. Silvestri, N. Barbani, G. Ciardelli, C. Cristallini, P. Giusti, Designing porous bioartificial membranes for clinical use with desired morphological and transport properties by phase inversion control, *J. Appl. Biomater. Biomech.* 3 (2005) 83–92.
- [20] L.M. Robeson, Polymer membranes for gas separation, *Curr. Opin. Solid State Mater. Sci.* 4 (1999) 549–552.
- [21] A.F. Ismail, R. Norida, A.R. Sunarti, Latest development on the membrane formation for gas separation, *Songklanakarin, J. Sci. Technol.* 24 (Suppl.) (2002) 1025–1043.
- [22] J. Ren, T.-S. Chung, D. Li, R. Wang, Y. Liu, Development of asymmetric 6FDA-2,6 DAT hollow fiber membranes for CO<sub>2</sub>/CH<sub>4</sub> separation. I. The influence of dope composition and rheology on membrane morphology and separation performance, *J. Membr. Sci.* 207 (2002) 227–240.
- [23] T.-S. Chung, S.K. Teoh, W.W.Y. Lau, M.P. Srinivasan, Effect of shear stress within the spinneret on hollow fiber membrane morphology and separation performance, *Ind. Eng. Chem. Res.* 37 (1998) 3930–3938.
- [24] T. Visser, G.H. Koops, M. Wessling, On the subtle balance between competitive sorption and plasticization effects in asymmetric hollow fiber gas separation membranes, *J. Membr. Sci.* 252 (2005) 265–277.

- [25] A. Bos, I.G.M. Punt, M. Wessling, H. Strathmann, CO<sub>2</sub>-induced plasticization phenomena in glassy polymers, *J. Membr. Sci.* 155 (1999) 67–78.
- [26] M. Wessling, M.L. Lopez, H. Strathmann, Accelerated plasticization of thin-film composite membranes used in gas separation, *Sep. Purif. Technol.* 24 (2001) 223–233.
- [27] S. Li, J.G. Martinek, J.L. Falconer, R.D. Noble, T.Q. Gardner, High-pressure CO<sub>2</sub>/CH<sub>4</sub> separation using SAPO-34 membranes, *Ind. Eng. Chem. Res.* 44 (2005) 3220–3228.
- [28] S.S. Dhingra, Mixed gas transport study through polymeric membranes: a novel technique, PhD Thesis, Department of Chemical Engineering, Virginia Polytechnic Institute and State University, USA, 1997, p. 146.
- [29] G. Xomeritakis, C.-Y. Tsai, C.J. Brinker, Microporous sol–gel derived aminosilicate membrane for enhanced carbon dioxide separation, *Sep. Purif. Technol.* 42 (2005) 249–257.
- [30] A.F. Ismail, N. Yaacob, Performance of treated and untreated asymmetric polysulfone hollow fiber membrane in series and cascade module configurations for CO<sub>2</sub>/CH<sub>4</sub> gas separation system, *J. Membr. Sci.* (2005) (on line).
- [31] L.J.P. van den Broeke, W.J.W. Bakker, F. Kapteijn, J.A. Moulijn, Binary permeation through a silicalite-1 membrane, *AIChE J.* 45 (1999) 976–985.
- [32] M. Ogawa, Y. Nakano, Separation of CO<sub>2</sub>/CH<sub>4</sub> mixture through carbonized membrane prepared by gel modification, *J. Membr. Sci.* 173 (2000) 123–132.